Soft-x-ray amplification in a laser-produced strontium plasma

C. J. Keane, D. L. Matthews, M. D. Rosen, T. W. Phillips, B. J. MacGowan, and B. L. Whitten
Lawrence Livermore National Laboratory, University of California, Livermore, California 94550

M. Louis-Jacquet, J. L. Bourgade, A. DeCoster, S. Jacquemot, D. Naccache, and G. Thiell
Centre d'Etudes de Limeil-Valenton, Boîte Postale No. 27, 94190 Villeneuve St. Georges, France
(Received 11 December 1989)

Amplification of soft x rays in Sr ($Z=38$) plasmas produced by second-harmonic laser irradiation of exploding foil targets is studied. Gains of 4.4 and 4.0 cm^{-1}, respectively, have been measured for the 164.1- and 166.5-Å $J=2$ to 1 transitions in Ne-like Sr at laser intensities of 1.3×10^{14} W/cm^2. Numerous x-ray and soft-x-ray transitions were identified in order to demonstrate typical spectra from x-ray laser plasmas and infer information regarding the plasma ionization balance. The $J=0$ to 1 transition at 159.8 Å, analogous to the well-known Se $J=0$ to 1 line at 182.4 Å, was not definitively observed due to a wavelength overlap with a Na-like Sr line. Two other $J=0$ to 1 transitions of interest at 84.9 and 133.0 Å were not observed. Reduced gain on the $J=2$ to 1 lasing lines was seen for several shots taken at a lower pump laser intensity of 7.0×10^{13} W/cm^2. Possible reasons for this are considered. The results of this work imply the feasibility of a high-output-power cavity geometry Ne-like Sr x-ray laser operating at 164.1 and 166.5 Å.

I. INTRODUCTION

Collisional excitation of Ne-like ions as a scheme for demonstrating x-ray lasing was first proposed and later refined throughout the 1970s.[1-3] Since the demonstration of soft x-ray amplification in Ne-like Se in 1984,[4,5] significant progress has been made in characterizing, isoelectronically scaling, and boosting the output power of Ne-like x-ray lasing systems. In particular, in plasmas produced by 0.53-μm light, up to 16 gain lengths have been observed in Ne-like Se (Refs. 6 and 7), and lasing has been demonstrated in Y ($Z=39$)[4] and Mo ($Z=42$).[8] In addition, gain in Ne-like Ge ($Z=32$),[9-11] Cu ($Z=29$),[9] Ga ($Z=31$),[12] As ($Z=33$),[12] and Se ($Z=34$)[12] has been reported in plasmas created by 1.06-μm-wavelength laser irradiation. Amplification has also been observed in Se (Ref. 13) in plasmas produced by 0.35-μm light. (An overview of progress in Ne-like x-ray lasers has been given in recent reviews.[14-16])

In this paper we present detailed spectroscopic measurements and the first measurement of soft-x-ray amplification in Ne-like Sr ($Z=38$). Sr was chosen as an element to study for several reasons. First of all, it is of interest from the point of view of Ne-like kinetics. Differences in the behavior of the gains of certain $J=0$ to 1 lines have been observed as a function of Z,[17] and hence it is of interest to attempt to measure gain on these $J=0$ to 1 transitions in as many different ions as possible. In addition, Sr is an ideal element from the point of view of x-ray laser applications. The bright $J=2$ to 1 lasing lines at 164.1 and 166.5 Å lie just on the long-wavelength side of the Si L absorption edge at 123 Å. Hence, they are in a wavelength range ideal for Mo and Si x-ray optics. Rapid progress in the fabrication of high-reflectivity multilayer structures in this wavelength region has been recently reported.[18-20] The recent demonstration of cavity operation of x-ray lasers[21] thus indicates that in principle a multipass Sr x-ray laser could provide a high brightness output at 164.1 and 166.5 Å. Such a laser could be useful in experiments such as x-ray holographic imaging[22] of dry-cell material and nonlinear x-ray optics.[23] Cavity operation of an x-ray laser may also allow x-ray amplifiers to be eventually pumped with much smaller optical lasers than those currently used. Finally, recent experiments by Monier *et al.*[24] have demonstrated fluorescence of the $2p^6$-$2p^5 3d$ line at 6.059 Å in Ne-like Sr due to photopumping of this transition by Ly-β emission at 6.053 Å in H-like Al. Photopumping may possibly be used to enhance the gain on transitions in the $3p$-$3s$ manifold (in particular, on several $J=0$ to 1 transitions[25]), and hence the measurement of gain in the nonphotoassisted case is of interest.

The remainder of this paper is divided into four sections. Section II describes the experimental setup, including laser and target conditions as well as the diagnostics used. The experimental results are presented and discussed in Secs. III and IV, respectively. Section V will summarize the results and conclusions of this work and will present directions for future research.

II. EXPERIMENTAL SETUP

The experiments described in this paper were carried out at the Phebus laser facility located at the Centre d'Etudes de Limeil-Valenton, France.[26] The facility is similar in overall plan to the Nova two-beam chamber.[8] Each of the two beams of the Phebus laser is identical to a single beam of the Nova laser facility at Lawrence Livermore National Laboratory. Pulse widths ranging from 100 ps to several nanoseconds and up to 5 TW per beam of power at the first harmonic are available. For these experiments, Phebus provided up to 1400 J/beam of

0.53-μm light in a 500-ps full width at half-maximum Gaussian pulse.

Figure 1 shows a schematic of the Phebus target chamber and associated diagnostics. The radius of this chamber is 130 cm, as compared to 80 cm for the Nova two-beam target chamber. The target was positioned at chamber center by a positioner capable of both translational and rotational movement. Each laser beam was focused onto the target by a pair of counterrotating cylindrical lenses and a single $f/4.3$ spherical lens. In this configuration a line focus continuously variable in length up to 2.7 cm was available. In an actual experiment, the line-focused beams were superimposed on the target; these beams were aligned using the alignment system shown in Fig. 1 and were colinear to within 1.5 mrad. Target foils of 0.8, 1.7, and 2.2 cm length were used in these experiments; the target foils were overfilled by the line focus in order to avoid effects arising from cold-edge plasmas. The alignment system for the targets was integral with that of the McPigs spectrometer (described below) and has been described previously.[8]

The diagnostics used in this work are also shown in Fig. 1. The two principal diagnostics used to record soft x-ray spectra and measure gain were a McPigs[27] (microchannel-plate intensified grazing incidence spectrometer) and a transmission-grating-streaked soft-x-ray spectrograph (Spartuvix).[28] The former provides high-resolution ($\Delta\lambda \sim 0.1-0.2$ Å) time-gated spectra, while the Spartuvix spectrograph yields continuous time resolution with reduced spectral resolution ($\Delta\lambda \sim 0.6$ Å).

The McPigs spectrometer operates at a 2° angle of incidence and utilizes gated microchannel plates with three cesium iodide–coated gold striplines to provide temporal resolution. In this case, each of the three individual striplines records soft-x-ray spectra starting before the laser pulse and up to a user-specified gate-off time. For this work, the three striplines were gated off at 300 ps, 1.5 ns, and 10 ns after the peak of the incident laser pulse. The alignment method for the McPigs spectrometer was as in previous work on the Nova two-beam laser and has been described elsewhere.[8] The spectrometer had an acceptance of 8 mrad in the horizontal direction and 0.4 mrad in the vertical; it was aligned colinear to the x-ray laser axis to within an accuracy of 1.5 mrad. As the expected geometric divergence for the output beam was 7 mrad, the McPigs spectrometer was aligned sufficiently precisely to view the whole x-ray laser plasma, with the spectrometer axis colinear with the direction of axial emission.

The Spartuvix spectrograph uses a streak camera in conjunction with a transmission grating to produce time-resolved measurements of soft-x-ray emission. Alignment of the Spartuvix diagnostic was done at the onset of the experimental campaign by aligning the instrument to the x-ray laser axis as defined by the target alignment system. (This alignment proved to be very stable; it was not necessary to align the Spartuvix spectrograph for each shot.) The Spartuvix diagnostic has a horizontal and vertical acceptance of 4 and 0.1 mrad, respectively. The diagnostic has a threshold detection level of 50 W/ster Å and a time resolution of 3 ps, and was capable of detecting x-ray laser emission from the shortest targets (0.8 cm) examined.

In addition to the Spartuvix and McPigs diagnostics that looked down the x-ray laser axis, a pair of streaked x-ray crystal spectrographs positioned off-axis were used to look at $n=3$ to 2 x-ray emission from these plasmas. Time-integrated x-ray crystal spectrometers were also employed. A set of time-integrated x-ray pinhole cameras (filtered to look in the 1.5-keV region) used to measure the line-focus width and verify beam superposition completed the diagnostic suite.

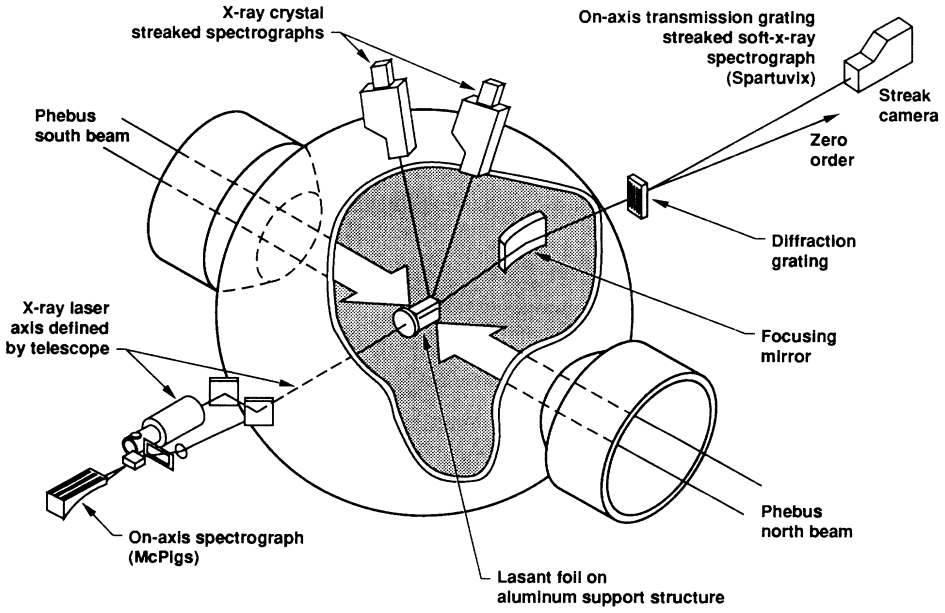

FIG. 1. Diagram of the Phebus target chamber and associated diagnostics.

III. EXPERIMENTAL RESULTS

The exploding-foil targets[5] employed in these experiments consisted of CH foils of areal density $10\mu g/cm^2$ overcoated with 80 $\mu g/cm^2$ of SrF_2. The majority of experiments were carried out at a nominal irradiance of 1.4×10^{14} W/cm^2. (All irradiances quoted in this paper are total, not per beam, values.) This intensity was derived from a simple scaling model for gain in Ne-like systems, and was estimated to be the optimum intensity for these targets.[29–31] This intensity is intermediate between the 7×10^{13} and 4×10^{14} W/cm^2 intensities used in previous work in Se (Refs. 4 and 5) ($Z=34$) and Mo (Ref. 8) ($Z=42$). The actual average measured intensity for this case was 1.3×10^{14} W/cm^2. The beam profile on target was observed to be uniform within 20% as measured by the x-ray pinhole cameras.

In addition, several shots were also carried out at a lower irradiance of 7×10^{13} W/cm^2. The 1.3×10^{14} W/cm^2 and 7.0×10^{13} W/cm^2 experiments will be referred to henceforth as the "high" and "low" irradiane cases. This pump-laser intensity variation was done in order to estimate the effect of pump-laser intensity on the observed spectra and measured gains. As precise variation of the laser energy was not possible over the limited number of shots available, the intensity was varied by setting the line-focus width to either 150 μm or 300 μm (full width at half maximum) for the high and low irradiance cases, respectively.

Figure 2 shows a simplified Grotrian diagram for Ne-like Sr and identifies the primary lasing transitions. [Note the $(2p_{3/2}3d_{5/2})_1$ level, which was the upper state pumped by the Al Ly-β line in the experiments of Monier *et al.*[24]] Based on previous results in Se (Refs. 4, 7, and 14) and Mo (Ref. 8), the two $J=2$ to 1 transitions at 164.1 and 166.5 Å are expected to have the highest gain. The three $J=0$ to 1 transitions shown in Fig. 2 are also of interest. The 84.9-Å transition shares the same upper level as the 159.8-Å $J=0$ to 1 line; measurement of gain on the 84.9-Å transition would thus yield information regarding the population of the $(2p_{1/2}3p_{1/2})_0$ level. (The line analogous to this at 113.4 Å in Ne-like Se has been observed, but no systematic attempts have been made to measure its gain.[32]) With respect to the 133.0-Å transition, gain has been observed on the corresponding line at 106.4 Å in Mo; observation of the analogous line in Se at 168.7 Å is complicated by the presence of a nearby Na-like Se transition.[32] Measurement of gain on the Sr 133.0-Å line should thus provide information on the Z scaling of $J=0$ to 1 gains, which could yield insight into issues such as the relatively weak amplification of certain $J=0$ to 1 transitions. In Fig. 2 the wavelengths of the 164.1- and 166.5-Å lines are taken from the work of Wyart *et al.*; a detailed listing of the sources for the wavelengths quoted in Fig. 2 is given in Table I. The description of the experimental results given below will be divided into a discussion of (a) soft-x-ray gain measurements and spectroscopy, and (b) x-ray spectroscopy.

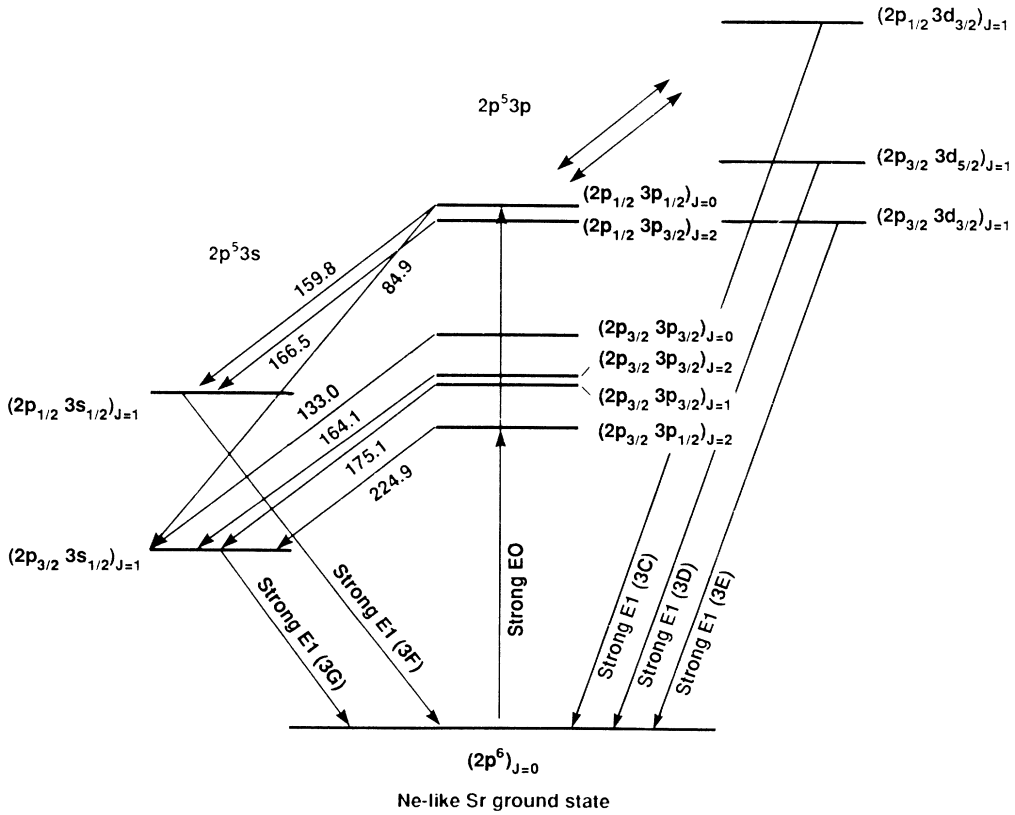

FIG. 2. Grotrian diagram for Ne-like Sr showing transitions of interest.

A. Soft-x-ray gain measurements and spectroscopy

Figure 3 shows a McPigs spectrum from a 2.2-cm-long SrF_2 target irradiated at a total intensity of 1.3×10^{14} W/cm^2. For this shot the spectrum was overexposed in order to allow weaker transitions to be viewed, and hence the relative intensities of various lines should not be used as an estimate of the gain-length product for a certain line. The principal lasing transitions shown in Fig. 2 are identified. The two $J=2$ to 1 transitions are observed to be the brightest lines in the spectrum, in accord with expectations. Two other bright Ne-like lines may be seen (the Se analogous wavelengths[14,33] appear in parentheses): the $J=1$ to 1 at 175.1 Å (220.8 Å) and the $J=2$ to 1 at 224.9 Å (262.94 Å). In the remainder of this section, we will first describe $J=2$ to 1 gain measurements and then turn to a discussion of detailed soft-x-ray spectroscopy; this will be followed by a summary of results concerning the three $J=0$ to 1 transitions shown in Fig 2.

Figure 4 shows the variation with target length of the intensity of the 164.1-Å transition as measured by the McPigs spectrometer for both the high- and low-intensity cases, along with inferred gain coefficients. In this figure the line intensity versus length has been fitted to the following formula:[34]

$$I=\frac{\epsilon}{\alpha}\frac{(e^{\alpha L}-1)^{3/2}}{(\alpha L e^{\alpha L})^{1/2}}\ , \tag{1}$$

where I is the intensity in W cm^{-2} ster^{-1} integrated over the line profile, α is the line-center gain coefficient, L is the target length, and ϵ is proportional to the emissivity. The two-parameter fit used yields values for α and ϵ. The gain curves are shown for both the high- and low-intensity experiments; the differing values for the gain in these cases will be discussed shortly. As can be seen from Fig. 4, the measured gains on the 164.1-Å line were 4.4 ± 0.5 cm^{-1} and 2.1 ± 0.6 cm^{-1} for the high- and low-intensity cases, respectively. The corresponding values for the 166.5-Å line were 4.0 ± 0.5 cm^{-1} and 1.1 ± 0.9 cm^{-1}. The gains and emissivities derived from the two-parameter fit to Eq. (1) are summarized in Table I. A discussion regarding the relative values of ϵ for the two $J=2$ to 1 lasing lines will be given in Sec. IV. Finally, in measuring the gains it was verified that the x-ray continuum scaled linearly with increasing target length, as has been observed in other exploding-foil Ne-like x-ray laser experiments.[4,8]

Figure 5 shows the measured time history of the 164.1-Å line from the Spartuvix diagnostic for a 2.2-cm-long target irradiated at high intensity. The observed duration of the laser emission is 182 ± 30 ps full width at half power. This is similar to the measured value of 170 ps for the Ne-like Se x-ray laser.[6,7,14] Time durations within 10% of this value were also measured for 1.7-cm-long targets irradiated at high intensity as well as for both 1.7- and 2.2-cm targets irradiated at low intensity. The emission time for 0.8-cm-long targets was 245 ± 30 ps and 200 ± 30 ps for the high- and low-intensity cases, respectively. The time history of the 166-Å emission was similar to that of the 164-Å line in all cases. It should be noted that measurements of the time history of lasing using diagnostics such as Spartuvix are affected by refraction.[6,7,14,36] The "sweeping" of the beam in the horizontal plane past the limited acceptance angle of the axial diagnostic results in the measured time duration being less

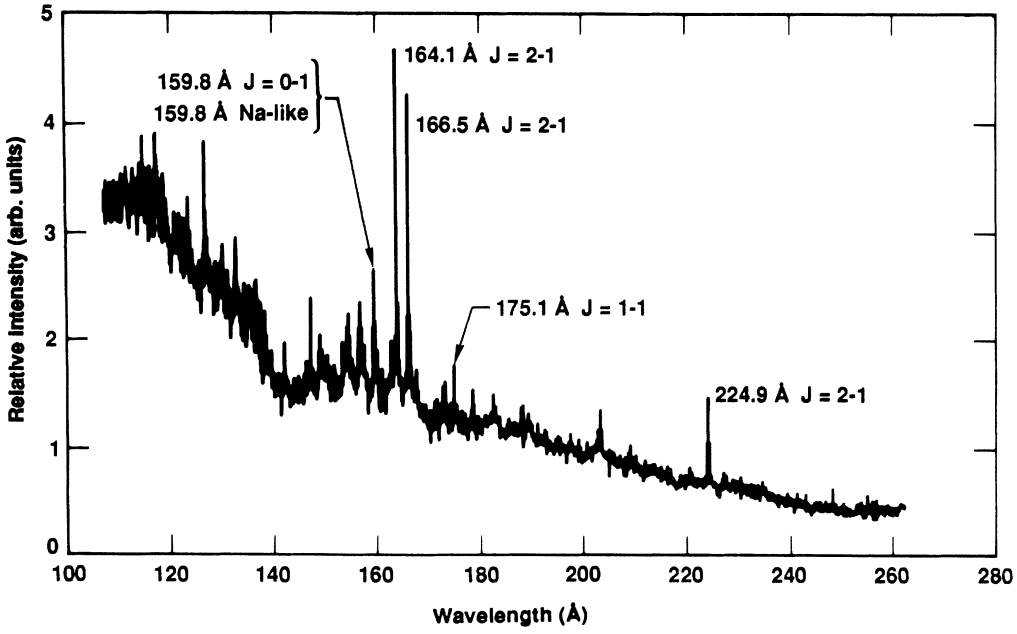

FIG. 3. Spectrum from a 2.2-cm-long SrF_2 foil irradiated at 1.3×10^{14} W/cm^2. The spectrum has been overexposed in order to allow weaker transitions to be viewed.

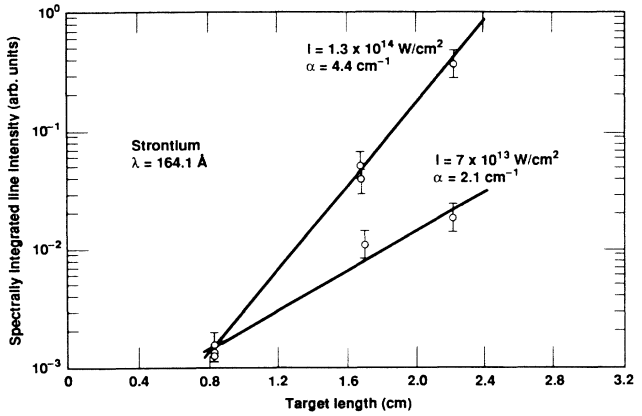

FIG. 4. Intensity of the Ne-like Sr 164.1-Å $J=2$ to 1 line vs target length for both the high- (1.3×10^{14} W/cm^2) and low- (6.0×10^{13} W/cm^2) irradiance cases.

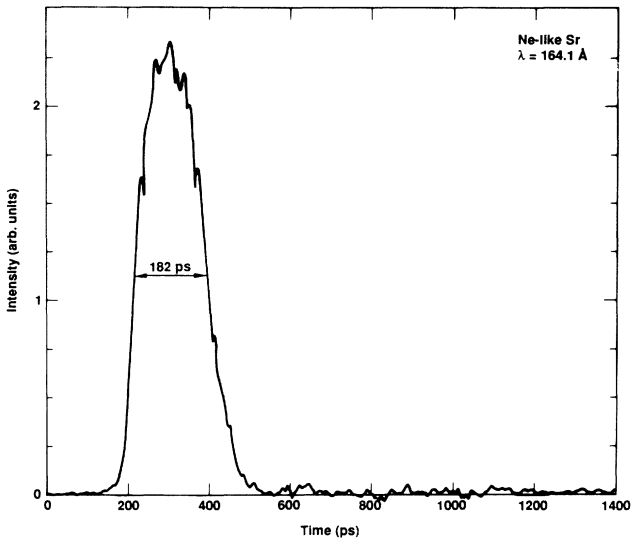

FIG. 5. Time history of the 164.1-Å line as measured by the Spartuvix diagnostic for a 2.2-cm-long target irradiated at high intensity.

than the actual value. In Se the true gain duration is closer to 400–500 ps.[37] A similar situation is expected to hold for Sr.

A definitive gain measurement was possible only for the two $J=2$ to 1 transitions. A two-point gain measurement of 1.0 cm^{-1} for the 224.9-Å line was obtained at high intensity, but the reliability of this measurement is low due to the weak level of line emission. The 175.1-Å line was observed for both high and low irradiance, but its intensity on shorter targets was too low to provide a reliable gain measurement. By analogy with previous work in Ne-like ions,[6,8,14] however, observation of the 224.9- and 175.1-Å transitions indicates that these lines were probably being amplified.

We now turn to a discussion of the soft-x-ray spectra observed from these plasmas. Figure 6 shows a late time (gate off at 10 ns) McPigs spectrum taken from a 0.8-cm-long SrF_2 target irradiated at 1.4×10^{14} W/cm^2. The wavelength scale shown in Fig. 6 was generated using previously reported lines of Mg- (Ref. 38), Na- (Refs. 39 and 40), and Ne- (Ref. 33) like Sr, Na- (Ref. 40) and Ne- (Ref. 8) like Mo, and Ne-like Ge (Ref. 9) as wavelength references. Polynomial fitting was used to derive a correction to the grating equation as a function of wavelength in order that the observed wavelengths of these reference lines would agree with the values published in the references above. The resulting error in the wavelengths of nonreference transitions as measured by the McPigs spectrometer is ±0.1 Å.

In a recent paper Wyart *et al.*[33] measured wavelengths for a variety of lines in Na-, Mg-, Al-, and Ne-like Sr. Comparison of the McPigs spectra with the line lists published by Wyart *et al.* yielded the identifications shown in Fig. 6. Note the large number of lines that originate from lower stages of ionization than Ne-like. In all cases, wavelengths of nonreference strontium lines agreed with those quoted by Wyart *et al.*[33] within the experimental uncertainty. In fact, the major significant difference between the spectrum in Fig. 6 and that of Wyart *et al.* is the increased intensity of the $J=2$ to 1 lasing lines. An

TABLE I. Summary table for transitions of interest in Ne-like Sr.

Transition	λ_{Sc}[a] (Å)	λ_{SR}[b] (Å)	α (cm^{-1})[c] High	α (cm^{-1})[c] Low	ϵ (arb. units)[c] High	ϵ (arb. units)[c] Low	Comment
$(2p_{1/2}3p_{1/2})_0$-$(2p_{3/2}3s_{1/2})_1$	113.43	84.88					Not observed
$(2p_{3/2}3p_{3/2})_0$-$(2p_{3/2}3s_{1/2})_1$	168.96	132.98					Not observed
$(2p_{1/2}3p_{1/2})_0$-$(2p_{1/2}3s_{1/2})_1$	182.44	159.80					No definite observation
$(2p_{3/2}3p_{3/2})_2$-$(2p_{3/2}3s_{1/2})_1$	206.42	164.1	4.4±0.5	2.1±0.6	3.4±3.0	10±10	
$(2p_{1/2}3p_{3/2})_2$-$(2p_{1/2}3s_{1/2})_1$	209.81	166.5	4.0±0.5	1.1±0.9	4.9±4.0	17±17	
$(2p_{3/2}3p_{3/2})_1$-$(2p_{3/2}3s_{1/2})_1$	220.31	175.1					Identified; too weak for gain measurement
$(2p_{3/2}3p_{1/2})_2$-$(2p_{3/2}3s_{1/2})_1$	262.94	224.9					Identified; too weak for gain measurement

[a]Wavelengths from Ref. 35.

[b]$J=2$ to 1 (164.1- and 166.5-Å) wavelengths measured and in agreement with Ref. 33; $J=0$ to 1 wavelengths from Ref. 32; $J=2$ to 1 (224.9-Å) and $J=1$ to 1 (175.1-Å) wavelengths measured and in agreement with Ref. 32. Accuracy of Sr wavelength measurements above ±0.1 Å.

[c]"High" and "Low" indicate experiments carried out at intensities of 1.3×10^{14} and 7.0×10^{13} W/cm^2, respectively.

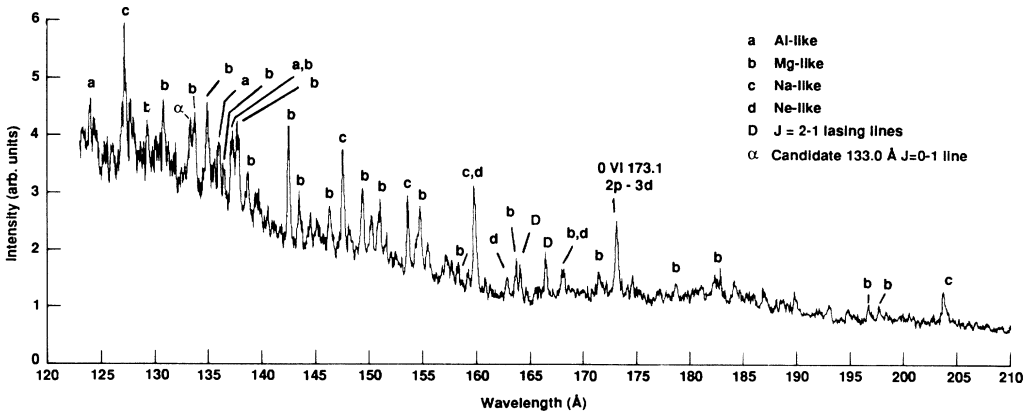

FIG. 6. Lineout of a soft-x-ray spectrum from the McPigs diagnostic for a 0.8-cm-long target irradiated at high intensity. Spectral features from various ion stages are shown. The feature marked α is near the correct position of the 133.0-Å $J=0$ to 1 line, but appears to originate from lower stages of ionization based on comparisons to the data of Wyart *et al.* (Ref. 33).

additional result to that shown in Fig. 6 is the identification of the nonlasing $(2p_{3/2}3p_{3/2})_1$-$(2p_{3/2}3d_{5/2})_2$ transition at 157.1 Å in Ne-like Sr. This line was observed on the stripline gated off at 300 ps on several shots. The line was not visible on striplines gated off at 1.5 ns and 10 ns (such as that shown in Fig. 6) due to the large late-time continuum (common to most Ne-like systems) that acts to obscure weak transitions.

With respect to the three $J=0$ to 1 transitions in Fig. 2, consider first the bright feature at 159.8 Å. This line represents a blend of the Na-like Sr $3p$-$3s$ 159.77-Å and Ne-like Sr 159.80-Å $J=0$ to 1 transitions. Due to the small wavelength difference, it was not possible to resolve spectrally the Na-like and Ne-like Sr transitions on the McPigs spectrometer. However, the 159.8-Å feature was observed to grow slower than linear on all McPigs time strips. For example, in lengthening the target from 0.8 cm to 1.7 cm the intensity of the 159.8-Å feature increased by a factor of 1.7 in the high-irradiance case and was unchanged for the low-irradiance case. It was also observed that the 159.8-Å linewidth was greater than the instrumental width of 0.27 Å for both intensities on all time strips. This type of behavior is well known for Na-like lines[6] and occurs because such lines are generally optically thick; indeed, this effect has been observed in Na-like Se lines.[37] Thus, based on the McPigs data, the 159.8-Å feature represents primarily Na-like emission. However, data from the Spartuvix spectrograph was suggestive of the Ne-like line being present at an early time. In particular, the time history of the 159.8-Å feature is different from that of other Na-like lines, showing a peak at early time coincident with the $J=2$ to 1 emission. However, the data are not sufficiently clear cut to render this a definitive observation of the $J=0$ to 1 transition.

Indeed, identification of the $J=0$ to 1 line for Sr is of some interest, as there is a possibility that any gain on the $J=0$ to 1 line may be suppressed due to absorption by the nearby 159.77-Å Na-like transition. Observation of an effect of this type would be of interest to understanding the issue of opacity, which is of importance for both x-ray lasers and general plasma spectroscopy. The Na-like wavelength of 159.77 Å was measured by Reader *et al.*[40] The current best extrapolated value for the wavelength of the Ne-like Sr $J=0$ to 1 transition is 159.80±0.05 Å.[32] Assuming $N_e=10^{21}$ cm^{-3}, $T_e=1$ keV, a Na-like Sr fraction of 20%, and Doppler broadening for the Na-like line, one finds that the absorption coefficient for the Na-like 159.77-Å transition is of order 3000 cm^{-1} at 159.80 Å, the calculated position of the $J=0$ to 1 line. At the outer limit of the error bar for the $J=0$ to 1 wavelength (159.85 Å), the absorption coefficient is closer to 1 cm^{-1}. Clearly, it appears as if absorption of the $J=0$ to 1 line by the Na-like Sr 159.77-Å line may be a significant effect. The use of a higher-resolution instrument capable of resolving these two transitions appears to be the best option available to identify the $J=0$ to 1 line and determine if any absorption effects are present. Such a measurement may be possible in the near future using an ultrahigh-resolution spectrometer designed to measure the linewidths of Ne-like lasing transitions.[41]

The other $J=0$ to 1 lines predicted to be at 84.9 and 133.0 Å were not observed. The wavelength region near 84.9 Å is relatively uncluttered and there was no evidence for the presence of this transition. The spectral region near 133.0 Å is quite crowded, however, as can be seen in Fig. 6. The lack of observation of the 133.0-Å line was substantiated by several observations. First, the spectrum in this region was very similar to that observed in the point-focus spectroscopy experiments of Wyart *et al.*[33] As the transitions observed by these authors were seen in spontaneous emission, this indicates that the lines in Fig. 6 near 133.0 Å also arose from spontaneous emission. (Recall that Ne-like lasing lines are generally very weak in spontaneous emission and only appear with significant intensity when amplified in line-focused produced plasmas.) There is an unidentified feature marked α in Fig. 6, but this was also observed by Wyart *et al.*, thus indicating it arises due to spontaneous emission, most probably from a lower stage of ionization such as Mg-like Sr. In addition, for the experiments discussed in this paper, feature α was observed to grow linearly with target length, as were the nearby 130.74-Å and 133.71-Å

Mg-like Sr transitions. Note that the absence of the 133.0-Å line is of interest, as the analogous transition at 106.4 Å in Mo has been observed to have a gain of 2.2 cm^{-1}. The implications of the lack of observation of the 84.9-Å and 133.0-Å lines will be discussed in Sec. IV. Table I summarizes the conclusions regarding the principal Ne-like Sr lines of interest in these experiments.

B. X-ray spectroscopy

X-ray spectra due to both $3\rightarrow2$ and $4\rightarrow2$ transitions in various Sr ion stages were also observed during these experiments. Figure 7 shows a time-integrated spectrum from a 2.2-cm-long SrF_2 foil for the high-intensity case. The film response has been removed from this data. Emission features from Na-, Ne-, F-, and O-like Sr are indicated. The x-ray spectra of Sr have been examined by several authors,[42–44] and the brightest Ne-like transitions are indicated in Fig. 7 using the standard $3A$, $3B$, etc, notation.

Several features in the spectra of Fig. 7 merit discussion. As an example, note the presence of the $2s$-$3d$ electric quadrupole line at 5.385 Å, first observed by Gauthier *et al.*[45] The ratio of this line to the $2s$-$3p$ Ne-like $3A$ transition has recently been demonstrated[46] to be an effective diagnostic of electron density in the case where it is possible to resolve in both time and space the emission of these two lines. Unfortunately, however, the time- and space-integrated nature of the spectrum shown in Fig. 7 prevents any reliable diagnostic interpretation of this line ratio. The $2s$-$3p$ F-like Sr features indicated in Fig. 7 have also been identified in these spectra. These lines have been identified previously in other ions;[47–49] in some cases, however, these features are mixed with O-like $2p$-$3d$ transitions.[50,51] In particular, the group of lines near 5.53 Å is composed of both F-like $2s$-$3p$ and O-like $2p$-$3d$ lines. (The features near 5.4 and 5.46 Å appear quite unambiguously to be F like.) However, assuming that line intensities are in proportion to their gf values and using the spectrum in the $4\rightarrow2$ region as a rough guide to the abundance of F- and O-like ions, one finds that at 5.53 Å the O-like $2p$-$3d$ emission dominates the F-like $2s$-$3p$ feature.

Indeed, spectral features from the Na-, Ne-, F-, and O-like Sr ions are better separated in the $4\rightarrow2$ than the $3\rightarrow2$ spectral region, and this makes unambiguous identification of emission from the latter two ion stages somewhat easier. An analysis of the spectrum in the $4\rightarrow2$ region can thus yield rough information regarding ionization balance. (Note that these lines are essentially optically thin.) In particular, it is of interest to compare the time-integrated spectra shown here with that obtained in other lasing elements such as Se and Mo, in order to estimate if similar plasma conditions are present. This comparison appears in Table II, where the relative abundances of Na-, Ne-, F-, and O-like ions are shown for the Sr experiments in this paper as well as for earlier experiments in Se and Mo. The relative abundances in Table II were obtained by varying the species abundances until good agreement with the experimental spectra in the $4\rightarrow2$ spectral region was obtained. Within an ion stage all lines were assumed to have an intensity proportional to their gf value; no detailed kinetics model is used. This technique in not meant to serve as an exact modeling of the experimental data and/or determination of the true ion relative abundances. Rather, when applied in a self-consistent way to spectra from different elements, this technique allows a rough comparison of the relative degree of ionization. Table II indicates that the relative abundance of the various Sr ion stages in time-integrated x-ray spectra is similar to that observed for Se. In addition, a comparison of the relative abundances agrees

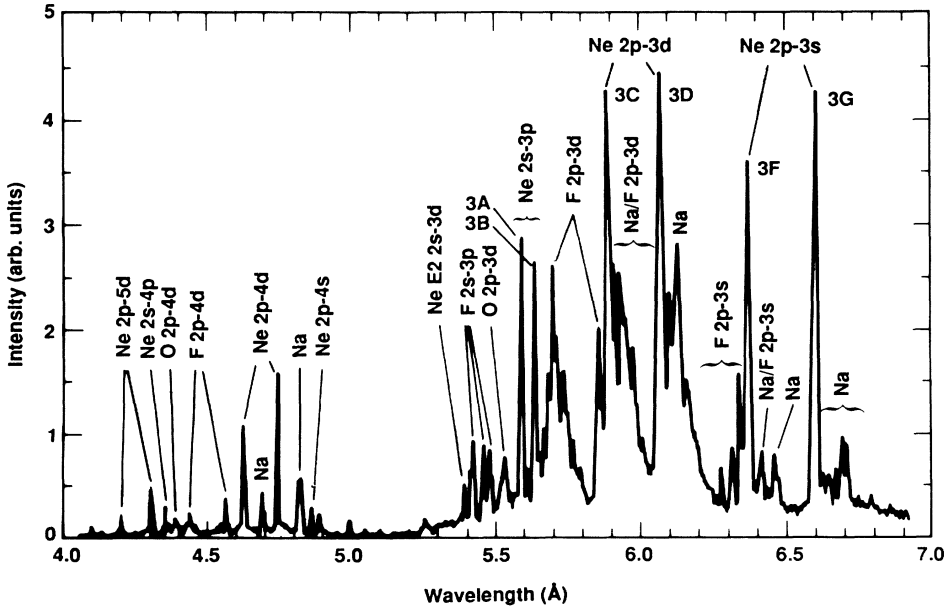

FIG. 7. Time-integrated x-ray spectrum taken from a 2.2-cm-long SrF_2 foil irradiated at high intensity.

TABLE II. Fractional abundances relative to the Ne-like stage based on gf-weighted relative line intensities. These measurements are based on time-integrated 4-2 x-ray spectra obtained under nominal target thickness (including CH backing) and irradiance conditions for each element: Se (45 $\mu g/cm^2$, 7×10^{13} W/cm^2 total), Mo (88 $\mu g/cm^2$, 4×10^{14} W/cm^2 total), Sr (high intensity) (90 $\mu g/cm^2$, 1.3×10^{14} W/cm^2 total). Results for the Sr low-intensity case are very similar to the Sr high-intensity results above.

Ion Stage	Se	Mo	Sr
Na-like	0.12	0.50	0.08
Ne-like	1.0	1.0	1.0
F-like	0.10	0.20	0.15
O-like	0.01	0.02	0.04

qualitatively with the broadening of the ionization balance as one proceeds to higher Z than is predicted by simple kinetics models.[31]

Time-resolved $3\rightarrow2$ x-ray spectra were also obtained in these experiments; the raw data from a 2.2-cm-long target irradiated at high intensity is shown in Fig. 8. In Fig. 9, a spectrum at time of peak emission from these data is shown. Figure 9 also shows an equivalent spectrum taken from a 1.7-cm-long target irradiated at low intensity. The main transitions of interest are identified. Note the strong similarity of these two spectra; the time histories for the high- and low-intensity cases are similarly equivalent. Indeed, comparison of the time-integrated data yields the same result; the line ratios are nearly identical for the high- and low-irradiance cases. (The similarity of the two cases is especially striking when compared to the solid Sr target spectra of Monier *et al.*[52] In this work, reduction of the irradiance from $3-5\times10^{14}$ to 1×10^{14} W/cm^2 resulted in a dramatic weakening relative to Ne-like line intensities of all the F-like Sr features in the spectrum.) This is evidence for the ionization balance being similar for the low- and high-intensity cases, a fact that we will return to in Sec. IV.

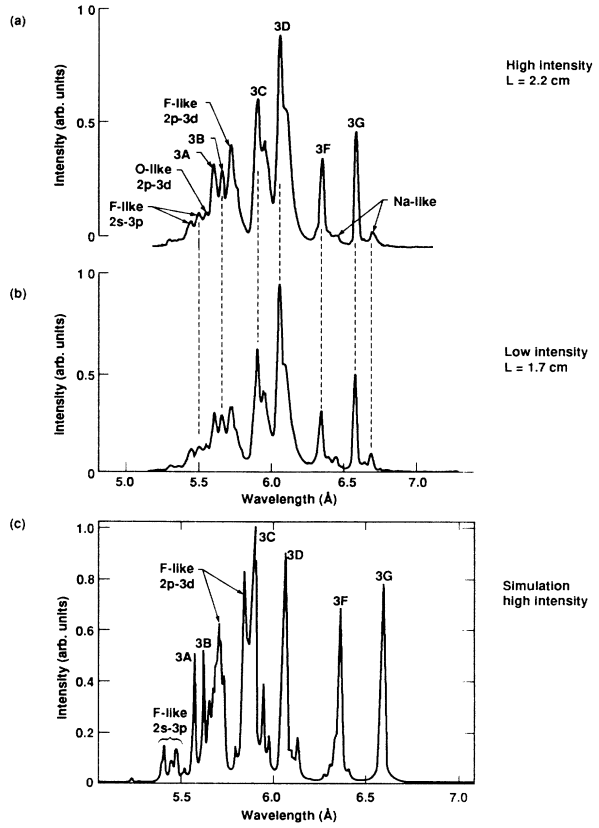

FIG. 9. Lineout of time-resolved x-ray spectra at peak emission time for (a) a 2.2-cm-long target irradiated at high intensity and (b) a 1.7-cm target irradiated at low intensity. (c) shows the simulated x-ray spectra taken at peak emission time for the case shown in Table III. Note that in the data in (a) and (b) the feature labeled 3*C* represents a combination of Ne-like and F-like Sr emission, as can be seen from Fig. 7.

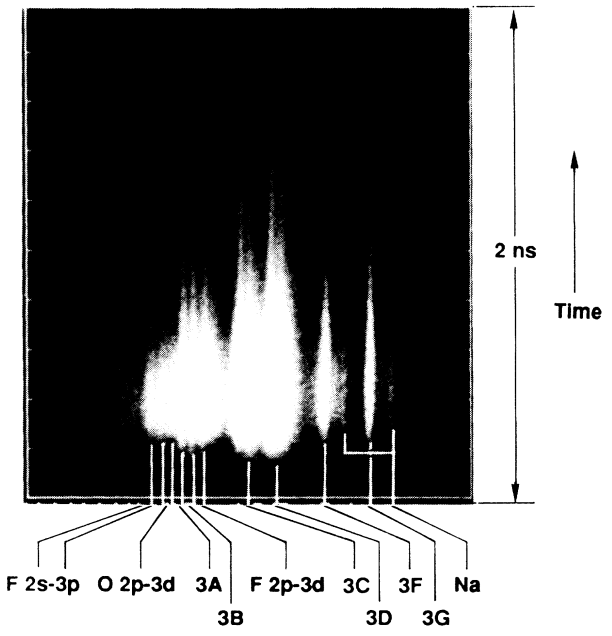

FIG. 8. Raw time-resolved x-ray data from a 2.2-cm-long SrF_2 foil irradiated at high intensity.

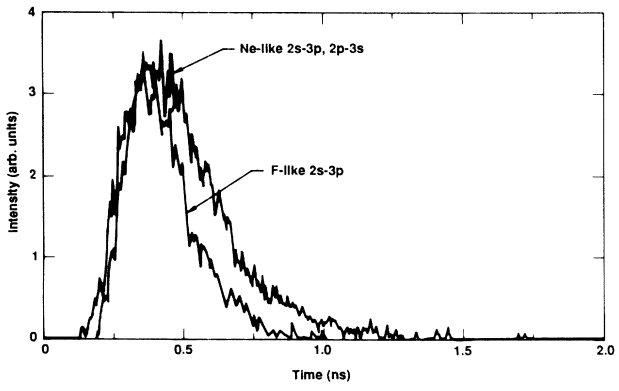

FIG. 10. Time histories of the Ne-like and F-like 2*s*-3*p* lines at 5.58 and 5.42 Å for a 2.2-cm-long SrF_2 target irradiated at high intensity.

A typical example of the time history of $3 \rightarrow 2$ x-ray emission for the high-irradiance case is shown in Fig. 10, where the time evolution of the Ne-like and F-like $2s$-$3p$ features at 5.58 and 5.42 Å are plotted. Note the slightly later start time and shorter duration of the F-like emission, as compared to the Ne-like emission. The observed behavior is consistent with the plasma ionizing during the laser pulse and peaking out in ionization near the F-like and O-like ion stages. In Sec. IV we discuss the implications of these time-integrated and time-resolved x-ray measurements in regard to the observed high and/or low irradiance variation in gain, and compare experimental results to simulation.

IV. DISCUSSION

The primary result of these experiments is the demonstration of gains of 4.4 and 4.0 cm^{-1} on the 164.1- and 166.5-Å $J=2$ to 1 lines in Ne-like Sr. Due to the relatively short wavelength of the lasing lines, the availability of high-reflectivity multilayer optics in the 165-Å spectral region, and the reasonable pump-laser intensities required, the Ne-like Sr x-ray laser is well suited for use in future applications work related to proof of principle experiments involving x-ray laser holography[22] and x-ray optics.[23]

Several features of the data merit further discussion. First, as discussed earlier, one of the observations in these experiments was the drop in the measured $J=2$ to 1 gain resulting from the lowering of the laser intensity from 1.3×10^{14} to 7×10^{13} W/cm^2. While further experiments are necessary to characterize this behavior fully, it is of interest to investigate the cause of what was observed. We have considered two possibilities for this behavior. These are (a) Ne-like kinetics effects due to the presumably cooler and denser plasmas produced at lower laser intensity, and (b) changes in x-ray laser propagation down the length of the amplifier due to the differing hydrodynamical conditions in the target produced by lower intensity irradiation. Below, we will discuss the implications of both the experimental data and detailed simulations in determining the relative importance of these two effects.

While the available data do not definitively confirm one or the other of these possibilities, x-ray and soft-x-ray spectra suggest that propagation effects are responsible for the reduced gain observed at lower irradiance. First, as discussed earlier, time-integrated and time-resolved x-ray spectra from low- and high-intensity targets show little overall difference in line ratios between Ne-, Na-, F-, and O-like lines. This would indicate that roughly similar ionization conditions are being produced in both the low- and high-intensity cases, and would thus tend to suggest that differences in plasma temperature and ionization balance are not responsible for the differing gains measured. (A more quantitative discussion of the observed x-ray spectra and their implication for the ionization balance is given below.) Note that opacity is not a major issue complicating this interpretation, largely due to relief of trapping due to bulk Doppler shifts.[53] In particular, while the optical depth of the $3D$ line is of order 10, that of the $3A$ and $3B$ lines is of order 1,and the F-like $2p$-$3d$ and $2s$-$3p$ transitions are essentially optically thin. Furthermore, time-integrated spectra in the $4 \rightarrow 2$ region (where the lines are also essentially optically thin) show little difference between the low- and high-intensity cases.

In a similar vein, the McPigs spectra as shown in Fig. 6 are very similar for the two irradiance cases. Thus, the observed x-ray and soft-x-ray spectra indicate that refraction may be responsible for the reduced gain. Definitive experimental demonstration of the presence of refraction (which has been observed previously in Ne-like Se x-ray laser experiments[6,7,14]) would require measurement of the Sr beam output pattern at both low and high intensities. In general, limited data are available at low irradiance; to characterize the low-intensity behavior of the gain will require further experiments. It should be noted that in general the focused pump-laser beam is not well characterized and that related unquantified effects (such as spatial variations of the pump-laser intensity) that affect the measured gains may be present.

We have also investigated the behavior of the gain in these targets from the theoretical viewpoint using one-dimensional LASNEX,[54] XRASER,[55] and SPECTRE simulations of these plasmas. The focus of these simulations is not to reproduce experimental measurements precisely, but to search for differential high and/or low intensity effects (such as refraction and/or changes in plasma conditions affecting the gain. The computational model used in these calculations is summarized as follows: Detailed excited-state structure is included for Ne- and F-like Sr, while excited levels of other ionization stages are treated hydrogenically. Dielectronic recombination from the F-like Sr ground state to excited levels of Ne-like Sr is included; for dielectronic recombination to other ion stages, only a single ground-state to ground-state rate is used. As with Se,[56] it is found that inclusion of dielectronic recombination effects in calculating the $J=2$ to 1 gains is important, as it enhances the computed $J=2$ to 1 gains by a factor of 2. Radiative transfer effects are also included in these simulations; effects of bulk Doppler shifts as discussed above are included in the local Sobolev approximation.[53] Inclusion of trapping effects lowers the computed gain coefficients by about 30% for both the low- and high-irradiance cases; it is thus an important ingredient in the analysis.

Simulations carried out under the nominal conditions used in the experiment showed the plasma to be strongly overionized and the gain increasing at lower irradiance, in contrast to observation. Hence, a modification[57] to the radiative loss factor in the simulations (resulting in lower plasma temperatures) applied to all cases considered was used to bring the calculated gains into qualitative agreement with measurements. (While this is an *ad hoc* method, the conclusions of the simulations regarding the relative importance of refraction and changes in plasma kinetics are basically independent of the modifying factor and corresponding span of plasma conditions.) Table III shows results from a sample calculation. Note that the calculated value of the expected gain for the 159.8-Å $J=0$ to 1 line is less than that for the $J=2$ to 1 transi-

TABLE III. Comparison of observations to simulations

Case	I (10^{14} W/cm^2)	Gain (cm^{-1}) 133 Å	159 Å	164 Å	166 Å	Peak T_e (keV)	F(%)	Ne (%)
Calculation[a]	1.4	1.6	4.1	7.0	6.0	1.2	40	35
	0.7	1.1	3.2	5.0	4.2	0.9	20	44
Data[b]	1.3			4.4	4.0			
	0.7			2.1	1.1			

[a]Quoted gain values are to be compared to McPigs measurements, i.e., they are time integrated and include effects of refraction.
[b]Gain values shown are identical to those in Table I and are derived from McPigs measurements.

tions. This does not represent changes in atomic data since earlier published results[5] show calculated $J=0$ to 1 gains to be greater than for the $J=2$ to 1 lines. Rather, the relatively smaller $J=0$ to 1 gains quoted here are due to refraction,[58,59] which discriminates more strongly in Sr than in Se against early-time high-gain $J=0$ to 1 emission arising from high-density, short-gradient scale-length regions. Finally, the calculated reduction in gain at low-irradiance is less than that observed; this may be due to errors in the kinetics model or other unknown factors.

A close study of this and other simulations run at both higher and lower intensities shows that the drop in the calculated gain at lower irradiance is due to the differing temperature and ionization conditions produced, and not from increased refraction arising from steeper density gradients. There is thus no evidence for a differential high-low irradiance refraction effect. Rather, in the simulations refraction is found to affect the high- and low-intensity cases similarly in two ways. First, it effectively reduces the net amplification at very early times when the gain is large and there are large density gradients present. Secondly, it results in an effective reduction of the local observed gain by 1.5 cm^{-1} at the time of peak measured gain. Neither of these two effects is a significant function of irradiance, and both are well-known effects that have been discussed previously for Ne-like Se.[58] Finally, simulations also indicate that the importance of bulk Doppler shifts implies that increased trapping arising due to the larger plasma size is not responsible for the reduced gains at low intensity. (Two-dimensional effects may modify this latter conclusion somewhat, however.) In summary, simulations indicate that the main effect of lowering the irradiance is to reduce the gain through changes in the plasma temperature and ionization balance.

Such changes in plasma conditions would be expected to be reflected in the calculated $3\rightarrow2$ spectra. Figure 9(c) shows the simulated $3\rightarrow2$ spectra for the high-intensity case given in Table III; note the good overall agreement with experiment. The data shown in Fig. 9(c) is thus consistent with the calculated ionization balance quoted in Table III. Simple estimates of the relative ion abundances based only on the data in Fig. 9(c) are also in reasonable agreement with the values quoted in Table III. It should be noted, however, that detailed absolute measurements of the ionization balance and plasma conditions from the data shown in Fig. 9(c) are model dependent; they thus carry some uncertainty due to the limited available spectral resolution (in particular, the lack of resolution of detailed Na-like satellite structure), as well as both the spatially integrated nature of the data and possible errors in a detailed atomic model. Such techniques have been discussed in detail elsewhere[46,60,61] and are beyond the scope of this paper. X-ray spectra such as those shown in Fig. 9(c) are thus best used as rough global monitors of plasma conditions and indicators of differential effects.

Calculations indicate that the major effect on the $3\rightarrow2$ time-resolved spectra of varying the irradiance is to lower the intensity of the F-like $2p$-$3d$ and $2s$-$3p$ features by a factor of 2–5 relative to the Ne-like lines. (The variation in this factor is due to variations in the *ad hoc* assumption discussed earlier.) This occurs due to the predicted reduced F-like Sr population at low irradiance. While the measurements presented in Fig. 9 do not show this effect, given the limited data set and uncertainty in measurements of such line ratios it is not unreasonable to postulate that a change of this order may not be seen in an actual experiment. Hence, while the available data suggest refraction effects are responsible for the reduced gain at lower irradiance, it does not rule out ionization balance and/or temperature changes as possible causes. Further experiments to verify and characterize the reduced gain at laser intensity are necessary before any firm conclusions can be drawn.

It can also be seen from Fig. 9(c) that the feature at 5.53 Å in the simulated spectrum is significantly weaker than the other F-like $2s$-$3p$ lines, which is not in accord with experiment. This due to the lack of O-like $2p$-$3d$ transitions in the model, and the simulated spectra thus provide additional evidence to support the identification of this feature in Fig. 7 as O-like, as discussed in Sec. III.

Similar results regarding the relative effects of refraction and changes in the ionization balance were obtained independently using the CHIVAS, LASIX, and OPTIQX (Ref. 62) suite of simulation codes. These calculations resulted in values close to those calculated by LASNEX and XRASER for peak gains. Analysis of refraction effects also yielded conclusions similar to those presented above.

Finally, a few two-dimensional calculations were also carried out. These simulations showed a reduced peak electron temperature for the high-intensity case due to two-dimensional conduction and expansion cooling effects. This resulted in only small differences between the peak electron temperatures and $3\rightarrow2$ spectra for the two irradiances as compared to the larger differences in the one-dimensional study. As a result of the similar

plasma conditions, the two-dimensional calculations also showed the gains to be very similar for the two intensities considered. As in the one-dimensional results, refraction was not found to affect the measured gains significantly. Hence, neither the one- nor the two-dimensional calculation showed a simultaneous reduction in gain and substantially unchanged $3\rightarrow 2$ spectra as a function of irradiance.

Another point of interest to examine is the relative values of the constants ϵ shown in Table I. The measured value of ϵ for a given line is proportional to the upper-state population N_u, transition probability $A_{u\text{-}l}$, source size, and emission time. As discussed earlier, the measured emission time is essentially identical for both $J=2$ to 1 lines and both irradiance cases. The values of ϵ shown in Table I are corrected for the factor-of-2 difference in source size between the high- and low-intensity cases arising from the different line-focus widths used. Hence, to first approximation the quoted values of ϵ are proportional to the product $N_u\ A_{u\text{-}l}$ for each line. Defining γ as the ratio of the constants ϵ for the 166.5- and 164.1-Å lines, it can be seen from Table I that γ is 1.4 and 1.7 for the high- and low-irradiance cases, respectively. The expected value of γ at the time of peak measured gain based on kinetics code calculations including all relevant levels in Ne-like Sr is 1.4 for both the high- and low-irradiance case.

Now, from the formula for small signal gain,

$$\alpha\ (\mathrm{cm}^{-1})=\frac{\lambda^2 A_{u\text{-}l}}{8\pi}\phi_\nu\left[N_u-\frac{g_u}{g_l}N_l\right], \tag{2}$$

it is apparent that if the lower-state population is negligible, then the gain on each transition is proportional to $N_u\ A_{u\text{-}l}$. [In Eq. (2), ϕ_ν is the line profile function.] Thus, should the lower-state populations be negligible, one would expect the gains of the 166.5- and 164.1-Å lines to be in the ratio γ. For the high-intensity case, the fact that the observed gains of the two $J=2$ to 1 lines are instead nearly equal [as also has been observed for Se (Refs. 6, 7, and 14) and Mo (Refs. 8 and 14)] thus suggests that the lower-state populations are critical in determining the gain. (At low intensity, the gains for the two $J=2$ to 1 lines are different, but in the opposite sense to that indicated by the measured values of ϵ. However, given the larger error bars, smaller gain values, and possible presence of refraction, it is not clear what importance to attach to this result.) This conclusion is consistent with kinetics models, which indicate both a value of 1.4 for γ and nearly identical $J=2$ to 1 gains. In summary, measurements suggest and calculations indicate that the lower-state population plays an important role in determining the gain on the $J=2$ to 1 transitions.

An additional important feature of these experiments was the lack of observation of the 133.0-Å $(2p_{3/2}3p_{3/2})_0$-$(2p_{3/2}3s_{1/2})_1$ Ne-like Sr transition. The lack of observation of this line in Sr, its relatively low calculated gain, and the measurement of a gain of 2.2 cm^{-1} on the analogous transition at 106.4 Å in Mo indicate that there is a significant Z scaling effect on the gain of this line. This is in accord with theoretical expectations based on the Z scaling of the electron monopole collisional excitation rate.[17] [Of course, the small gains on the $(2p_{1/2}3p_{1/2})_0$-$(2p_{1/2}3s_{1/2})_1$ transitions measured in Se (Refs. 6, 7, and 14) and Mo (Refs. 8 and 14) are not consistent with theory.] To recap the status of the other $J=0$ to 1 lines, as discussed in Sec. III, neither the 159.80- or 84.9-Å transitions were observed; identification of the former was hampered by an overlap with a Na-like Sr transition at 159.77 Å. We plan to investigate further the Z scaling of $J=0$ to 1 lines in future experiments.

V. CONCLUSIONS

In this paper we have presented measurements of gain on several soft-x-ray transitions in Ne-like Sr. Gains of 4.4 and 4.0 cm^{-1} were measured for the 164.1-Å and 166.5-Å $J=2$ to 1 transitions at pump-laser intensities of 1.3×10^{14} W/cm^2. Several shots carried out at a lower irradiance of 7×10^{13} W/cm^2 were consistent with reduced gains of 2.1 and 1.1 cm^{-1} for the 164.1- and 166.5-Å lines. The 175.1- and 224.9-Å transitions were observed, but line intensities were too weak to provide a definitive measurement of gain for either. Evidence for observation of the $J=0$ to 1 line at 159.80 Å was seen in time-resolved data, but definitive identification of the line was not possible due to a wavelength overlap with a nearby Na-like Sr transition at 159.77 Å. Simple estimates indicate that any gain on the 159.80-Å line may be suppressed due to absorption by this Na-like Sr transition. Neither the 84.9-Å or the 133.0-Å $J=0$ to 1 transition was observed. Based on this data and previous work in Se and Mo, we conclude that there is a Z-scaling effect present for the gain on the $(2p_{3/2}3p_{3/2})_0$-$(2p_{3/2}3s_{1/2})_1$ line.

Time-integrated and time-resolved x-ray spectra indicated that plasmas of similar degrees of ionization were being produced in the high- and low-intensity experiments. The available data suggest that refraction may be responsible for the lower gain measured at lower irradiance. While confirming the importance of refraction in general, detailed LASNEX-XRASER-SPECTRE simulations imply that the reduced level of ionization and lower temperature are responsible for the decrease in gain for the lower irradiance case. Only limited data are available at low irradiance, but then suggest that the expected change in the low-intensity $3\rightarrow 2$ x-ray spectra corresponding to these changes in plasma conditions was not observed. Further experiments and modeling are required in order to verify and understand fully the variation of gain with intensity.

In summary, these experiments have contributed a number of interesting observations to our knowledge base regarding Ne-like systems. These measurements should aid in efforts to understand the physics of gain production in Ne-like ions.

ACKNOWLEDGMENTS

We would like to express our appreciation to the Phebus operations crew for their outstanding work during the entire series of joint Lawrence Livermore Nation-

al Laboratory–Centre d'Etudes de Limeil-Valenton x-ray laser experiments. In addition, we would like to thank the following LLNL personnel for their contributions: D. Nilson, G. Stone, J. Cox, and S. Brown for their efforts in diagnostic and target preparation; R. London for discussions on refraction; and J. Nash for constructing the Sr model used in the calculations. We acknowledge a productive discussion with J. F. Wyart at the University of Paris, Orsay. C. Pearson of Colorado College is to be thanked for his assistance in data analysis. This work was performed under the auspices of the U.S. Department of Energy by the Lawrence Livermore National Laboratory under Contract No. W-7405-ENG-48.

---

[1]A. N. Zherikhin, K. N. Koshelev, and V. S. Letokhov, Kvant. Elektron. (Moscow) **3**, 152 (1976) [Sov. J. Quantum Electron. **6**, 82 (1976)].

[2]A. V. Vinogradov, I. I. Sobel'man, and E. A. Yukov, Kvant. Elektron. (Moscow) **4**, 63 (1977) [Sov. J. Quantum Electron. **7**, 32 (1977)].

[3]A. V. Vinogradov and V. N. Shlaptsev, Kvant. Elektron. (Moscow) **10**, 2325 (1983) [Sov. J. Quantum Electron. **13**, 1511 (1983)], and references therein.

[4]D. L. Matthews *et al.*, Phys. Rev. Lett. **54**, 110 (1985).

[5]M. D. Rosen *et al.*, Phys. Rev. Lett. **54**, 106 (1985).

[6]D. L. Matthews, M. D. Rosen, S. B. Brown, N. M. Ceglio, D. C. Eder, A. M. Hawryluk, C. J. Keane, R. A. London, B. J. MacGowan, S. Maxon, D. G. Nilson, J. H. Scofield, and J. E. Trebes, J. Opt. Soc. Am. B **4**, 575 (1986).

[7]B. J. MacGowan, S. Brown, E. M. Campbell, M. Eckart, P. Hagelstein, C. Keane, R. London, D. Matthews, D. Nilson, T. Phillips, M. Rosen, J. Scofield, G. Shimkaveg, A. Simon, R. Stewart, J. Trebes, D. Whelan, D. Whitten, and J. Woodworth, Soc. Photo-Opt. Instrum. Eng. **688**, 36 (1986).

[8]B. J. MacGowan, M. D. Rosen, M. J. Eckart, P. L. Hagelstein, D. L. Matthews, D. G. Nilson, T. W. Phillips, J. H. Scofield, G. Shimkaveg, J. E. Trebes, R. S. Walling, B. L. Whitten, and J. G. Woodworth, J. Appl. Phys. **61**, 5243 (1987).

[9]T. N. Lee, E. A. McLean, and R. C. Elton, Phys. Rev. Lett. **59**, 1185 (1987).

[10]M. Louis-Jacquet, J. L. Bourgade, P. Combis, S. Jacquemot, J. P. Le Breton, D. Naccache, J. P. Perrine, and O. Peyrusse, C. R. Acad. Sci. **306**, Series II, 867 (1988).

[11]C. L. S. Lewis (private communication).

[12]T. N. Lee, E. A. McLean, J. A. Stamper, H. R. Griem, and C. K. Manka, Bull. Am. Phys. Soc. **33**, 1920 (1988).

[13]C. J. Keane, B. J. MacGowan, D. L. Matthews, R. A. London, S. Maxon, M. D. Rosen, J. L. Bourgade, A. DeCoster, S. Jacquemot, M. Louis-Jacquet, and D. Naccache, Appl. Phys. B **50**, 257 (1990); C. J. Keane, J. L. Bourgade, P. Combis, R. A. London, M. Louis-Jacquet, B. J. MacGowan, D. L. Matthews, D. Naccache, O. Peyrusse, M. D. Rosen, G. Thiell, and B. Whitten, in *OSA Proceedings on Short Wavelength Coherent Radiation: Generation and Applications,* edited by R. Falcone and J.Kirz (Optical Society of America, Washington, DC, 1989), Vol. 2.

[14]C. J. Keane, N. M. Ceglio, D. L. Matthews, B. J. MacGowan, D. G. Nilson, J. E. Trebes, and D. A. Whelan, J. Phys. B **22**, 3343 (1989).

[15]R. A. London, M. D. Rosen, S. Maxon, and D. C. Eder, J. Phys. B **22**, 3363 (1989).

[16]B. J. MacGowan, J. L. Bourgade, P. Combis, C. J. Keane, R. A. London, M. Louis-Jacquet, D. L. Matthews, S. Maxon, D. Naccache, M. D. Rosen, G. Thiell, and D. A. Whelan, in *OSA Proceedings on Short Wavelength Coherent Radiation: Generation and Applications,* edited by R. Falcone and J. Kirz (Optical Society of America, Washington, DC, 1989).

[17]B. L. Whitten, M. H. Chen, A. U. Hazi, C. J. Keane, R. A. London, B. J. MacGowan, D. L. Matthews, T. W. Phillips, M. D. Rosen, J. L. Trebes, and D. A. Whelan, in *Proceedings of the International Conference on Lasers '88, Lake Tahoe, NV, 1988,* edited by R. S. Sze and F. J. Duarte (STS Press, McLean, VA, 1989).

[18]N. M. Ceglio, in *X-ray Microscopy II,* edited by D. Sayre, M. Howells, J. Kirz, and H. Rarback (Springer-Verlag, NY, 1988), p. 130.

[19]A. M. Hawryluk, N. M. Ceglio, and D. G. Stearns, J. Vac. Sci. Technol. B **6**, 2153 (1988).

[20]D. G. Stearns, N. M. Ceglio, A. M. Hawryluk, M. B. Stearns, A. K. Retford-Long, C. H. Chang, K. Danzmann, M. Kuhne, P. Muller, and B. Wende, Proc. Soc. Photo-Opt. Instrum. Eng. **688**, 91 (1986).

[21]N. M. Ceglio, D. G. Stearns, D. P. Gaines, A. M. Hawryluk, and J. E. Trebes, Opt. Lett. **13**, 108 (1987).

[22]J. E. Trebes, S. B. Brown, E. M. Campbell, D. L. Matthews, D. G. Nilson, G. F. Stone, and D. A. Whelan, Science **238**, 517 (1987).

[23]N. M. Ceglio, in *OSA Proceedings on Short Wavelength Coherent Radiation: Generation and Applications,* edited by R. Falcone and J. Kirz (Optical Society of America, Washington, DC, 1989), Vol. 2.

[24]P. Monier, C. Chenais-Popovics, J. P. Geindre, and J. C. Gauthier, Phys. Rev. A **38**, 2508 (1988).

[25]M. D. Rosen and D. L. Matthews, Bull. Am. Phys. Soc. **33**, 2042 (1988).

[26]G. Thiell, A. Adolf, M. Andre, N. Fleurot, D. Friart, P. Juraszek, and D. Schirmann, Lasers and Particle Beams **6**, 93 (1988).

[27]M. J. Eckart and N. M. Ceglio, in *Energy and Technology Review,* LLNL Publication No. UCRL-52000-85-11 (Lawrence Livermore National Laboratory, Livermore, CA), 1985 (unpublished), p. 25.

[28]J. L. Bourgade, P. Combis, M. Louis-Jacquet, J. P. LeBreton, J. de Mascureau, D. Naccache, R. Sauneuf, G. Thiell, C. J. Keane, B. J. MacGowan, and D. L. Matthews, Rev. Sci. Instrum. **59**, 1840 (1988).

[29]R. A. London and M. D. Rosen, Phys. Fluids **29**, 3813 (1986).

[30]M. D. Rosen, R. A. London, and P. L. Hagelstein, Phys. Fluids **31**, 666 (1988).

[31]B. L. Whitten, R. A. London, and R. S. Walling, J. Opt. Soc. Am. B **5**, 2537 (1988).

[32]J. Scofield (private communication).

[33]J. F. Wyart, J. C. Gauthier, J. P. Geindre, N. Tragin, P. Monier, A. Klisnick, and A. Carillon, Phys. Scr. **36**, 227 (1987).

[34]G. J. Linford, E. R. Peressini, W. R. Sooy, and M. L. Spaeth, Appl. Opt. **13**, 379 (1974).

[35]M. J. Eckart, H. H. Scofield, and A. U. Hazi, in Proceedings

of the International Colloquium on UV and X-ray Spectroscopy, Beaulieu-sur-Mer, France, 1987 [J. Phys. (Paris) Colloq. **49**, C1-361 (1988)].

[36]M. D. Rosen, J. E. Trebes, B. J. MacGowan, P. L. Hagelstein, R. A. London, D. L. Matthews, D. G. Nilson, T. W. Phillips, D. A. Whelan, G. Charaitis, G. E. Busch, C. L. Shepard, and V. L. Jacobs, Phys. Rev. Lett. **59**, 2283 (1987).

[37]B. J. MacGowan *et al.* (unpublished).

[38]J. Reader, J. Opt. Soc. Am. B **73**, 796 (1983).

[39]J. Reader, J. Opt. Soc. Am. B **3**, 870 (1986).

[40]J. Reader, V. Kaufman, J. Sugar, J. O. Eckberg, U. Feldman, C. M. Brown, J. F. Seely and W. L. Rowan, J. Opt. Soc. Am. B **4**, 1821 (1987).

[41]M. C. Hettrick, J. H. Underwood, P. J. Batson, and M. J. Eckart, Appl. Opt. **27**, 200 (1988); M. C. Hettrick and J. H. Underwood, in *Short Wavelength Coherent Radiation: Generation and Applications* (Monterey, CA, 1986) AIP Conf. Proc. No. 147, edited by D. Attwood and J. Bokor (AIP, New York, 1986), p. 237.

[42]R. J. Hutcheon, L. Cooke, M. H. Key, C. L. S. Lewis, and G. E. Bromage, Phys. Scr. **21**, 89 (1980).

[43]H. Gordon, M. G. Hobby, N. J. Peacock, and R. D. Cowan, J. Phys. B **12**, 881 (1979).

[44]J. C. Gauthier, J. P. Geindre, P. Monier, C. Chenais-Popovics, J. F. Wyart, and E. Luc-Koenig, in *Proceedings of the Third International Conference on Radiative Properties of Hot Dense Matter,* edited by B. Rozsnyai, C. Hooper, R. Cauble, R. Lee, and J. Davis, (World Scientific, Singapore, 1987), p. 154.

[45]J. C. Gauthier, J. P. Geindre, P. Monier, E. Luc-Koenig, and J. F. Wyart, J. Phys. B **19**, L385 (1986).

[46]B. K. F. Young, A. L. Osterheld, R. S. Walling, W. H. Goldstein, T. W. Phillips, R. E. Stewart, G. Charaitis, and Gar. E. Busch, Phys. Rev. Lett. **62**, 1266 (1989).

[47]H. Gordon, M. G. Hobby, and N. J. Peacock, J. Phys. B **13**, 1985 (1980).

[48]L. F. Chase, W. C. Jordan, J. D. Perez, and R. R. Johnston, Phys. Rev. A **13**, 1497 (1976).

[49]J. F. Seely, T. W. Phillips, R. S. Walling, J. Bailey, R. E. Stewart, and J. H. Scofield, Phys. Rev. A **34**, 2942 (1986).

[50]P. G. Burkhalter, G. A. Doschek, U. Feldman, and Robert D. Cowan, J. Opt. Soc. Am. **67**, 741 (1977).

[51]P. G. Burkhalter, R. Schneider, C. M. Dozier, and Robert D. Cowan, Phys. Rev. A **18**, 718 (1978).

[52]P. Monier, Ph.D. thesis, University of Paris, Orsay, France, 1988.

[53]Y. T. Lee, R. A. London, G. B. Zimmerman, and P. L. Hagelstein, Phys. Fluids B (to be published).

[54]G. B. Zimmerman and R. M. More, Comments Plasma Phys. Controlled Fusion **2**, 51 (1975).

[55]P. L. Hagelstein, Lawrence Livermore National Labortory Report No. UCRL-53100, 1981 (unpublished).

[56]M. D. Rosen and P. L. Hagelstein, in *Short Wavelength Coherent Radiation: Generation and Applications (Monterey, CA, 1986),* AIP Conf. Proc. No. 147, edited by D. T. Attwood and J. Bokor (AIP, New York, 1986), p. 110.

[57]S. Maxon, S. Dahled, P. L. Hagelstein, R. A. London, B. J. MacGowan, M. D. Rosen, G. Charatis, and G. Busch, Phys. Rev. Lett. **63**, 236 (1989); **63**, 1896 (1989).

[58]R. A. London, Phys. Fluids **31**, 184 (1988).

[59]M. D. Rosen *et al.*, in *Atomic Processes in Plasmas,* Proceedings of a Conference on Atomic Processes in Plasmas, Santa Fe, New Mexico, 1987, AIP Conf. Proc. No. 168, edited by A. Hauer and A. Merts (AIP, New York, 1988), p. 102.

[60]W. Goldstein, R. Walling, J. Bailey, M. Chen, R. Fortner, M. Klapisch, T. Phillips, and R. Stewart, Phys. Rev. Lett. **58**, 2300 (1987).

[61]O. Peyrusse, P. Combis, M. Louis-Jacquet, D. Naccache, C. J. Keane, B. J. MacGowan, and D. L. Matthews, J. Appl. Phys. **65**, 3802 (1989).

[62]M. Louis-Jacquet, J. L. Bourgade, J. Bruneau, P. Combis, J. P. Jadaud, J-P. Le Breton, D. Naccache, G. Nierat, J-P. Perring, G. Thiell, A. Decoster, S. Jacquemot, O. Peyrusse, C. J. Keane, D. L. Matthews, and B. J. MacGowan, Centre d'Etudes de Limeil-Valenton Report DAM/CEL-V/DLPP/EPL No. 173/88, 1988 (unpublished).

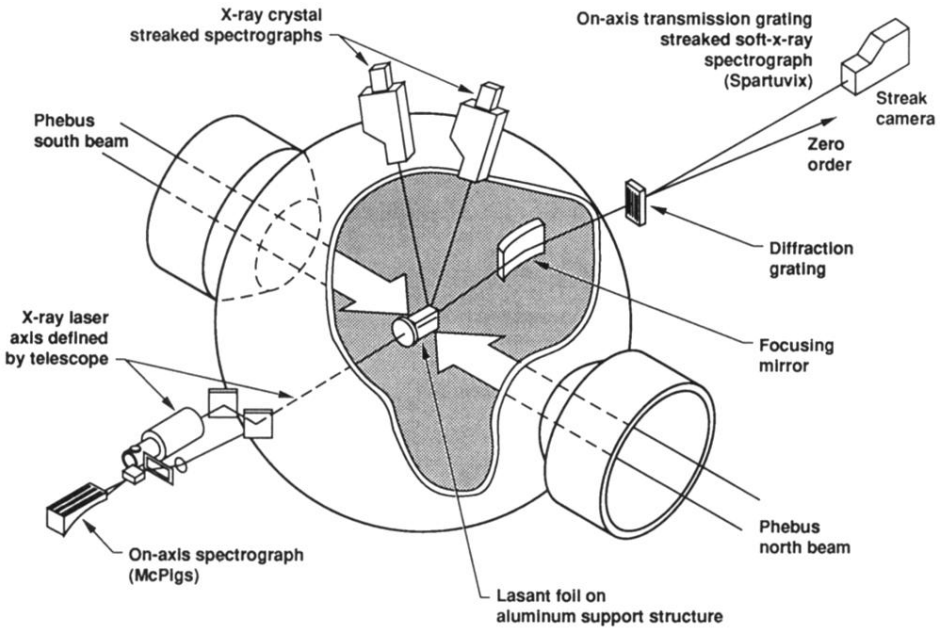

FIG. 1. Diagram of the Phebus target chamber and associated diagnostics.

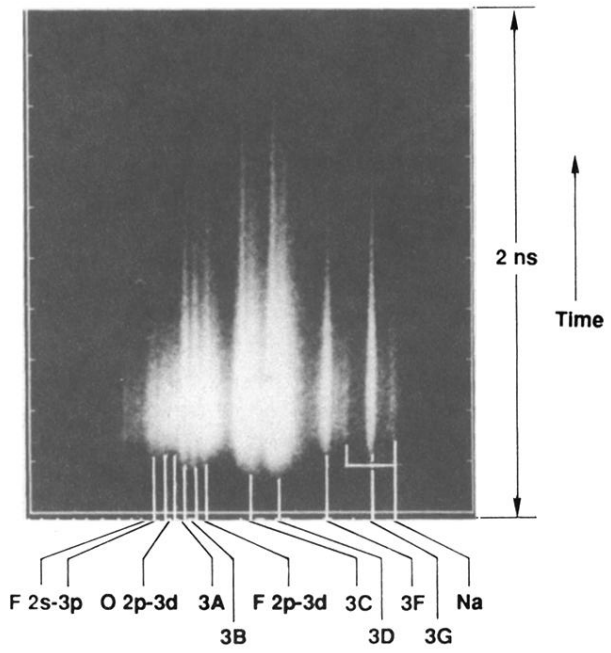

FIG. 8. Raw time-resolved x-ray data from a 2.2-cm-long SrF_2 foil irradiated at high intensity.